First experimental results of a new free liquid piston Ericsson engine

Ryma Chouder[a], Max Ndamé Ngangué[b], Pascal Stouffs[c] and Azzedine Benabdesselam[d]

[a] Universite de Pau et des Pays de l'Adour, E2S UPPA, LaTEP, Pau, France, rchouder@univ-pau.fr
[b] Laboratoire de Technologie et de Sciences Appliquées, IUT de l'Université de Douala, Cameroun, maxndame@yahoo.fr
[c] Universite de Pau et des Pays de l'Adour, E2S UPPA, LaTEP, Pau, France, pascal.stouffs@univ-pau.fr, Corresponding Author
[d] Laboratoire des Transports Polyphasiques et Milieux Poreux (LTPMP), FGPGM, USTHB, Algiers, Algeria, benabdesselam2000@yahoo.com

Abstract:

A new Ericsson free-liquid-piston engine (FLPEE) configuration was previously presented. This consists of a U-shaped tube filled with water in its lower part, and whose two branches are closed by cylinder heads fitted with valves. The space between the surface of the liquid and the cylinder head of one of the branches constitutes the compression space, while this same space constitutes the expansion space in the other branch. The configuration studied operates in an open cycle. This system is able to produce compressed air which can be expanded in an external device to produce mechanical energy. This FLPEE is thought to be suited for the conversion of thermal energy such as solar energy, biomass or flue gases. In this communication, the experimental bench is presented in detail. In particular, the valve control system of the compression and expansion spaces, the various sensors and the data acquisition system are described. Various experimental results are presented, notably in the form of (p, V) indicator diagrams of the compression and expansion cylinders. These results confirm what the theoretical modelling had predicted, namely that it is possible to obtain a set of values of the operational parameters of the system leading to a stable operation of the free-piston system.

Keywords:

Free piston engine; Ericsson engine; Liquid piston, Experimental results.

1. Introduction

External heat engines such as Stirling or Ericsson engines [1] are proving to be a relevant technological solution for the valorisation of thermal energy such as solar energy, the energetic valorisation of hot gaseous effluents or the combustion of biomass, in order to produce low power mechanical or electrical energy. A major advantage of Ericsson engines over Stirling engines is that the heat exchangers are not dead volumes and can therefore be sized solely on heat transfer considerations [2]. This is particularly interesting in the case of hot sources with relatively low temperature or low transfer coefficient, such as flue gases. However, with regard to Ericsson engines, despite their interest and numerous theoretical developments [3-7], there is still little experimental work.

Liquid piston machines are particularly interesting because they ensure a perfect seal between the piston and the cylinder, while drastically reducing frictional forces. In addition, they can considerably improve heat transfer with the working fluid, for example to approach isothermal compression [8-10].

Free piston engines do not require a crank-connecting rod arrangement to transform reciprocating motion into rotary motion. Mechanical losses are therefore lower and the cost of the engine is reduced [11]. There are free piston internal combustion engines [12-15] or free piston Stirling engines [16-18] and free liquid piston Stirling engines, also known as Fluidyne. These engines, developed for pumping applications, have a poor efficiency [19-20].

In this paper, a totally new engine configuration combining the advantages of Ericsson engines, liquid piston machines and free piston engines is studied [21]. Dynamic simulation results of this engine have shown that it is possible to design a free liquid piston Ericsson engine (FLPEE) which, combined with a judicious choice of operational parameters, allows stable operation with interesting energy performance [22]. In particular, the FLPEE has a much better energy performance than the Fluidyne, which is the most similar configuration.

https://doi.org/10.52202/069564-0062

An experimental bench is being developed to validate the theoretical results. This bench is described and the first results are presented.

2. The test bench

2.1. The configuration under consideration

The configuration studied (Figure 1) consists of a U-shaped tube filled with water in its lower part, and whose two branches are closed by cylinder head fitted with valves.

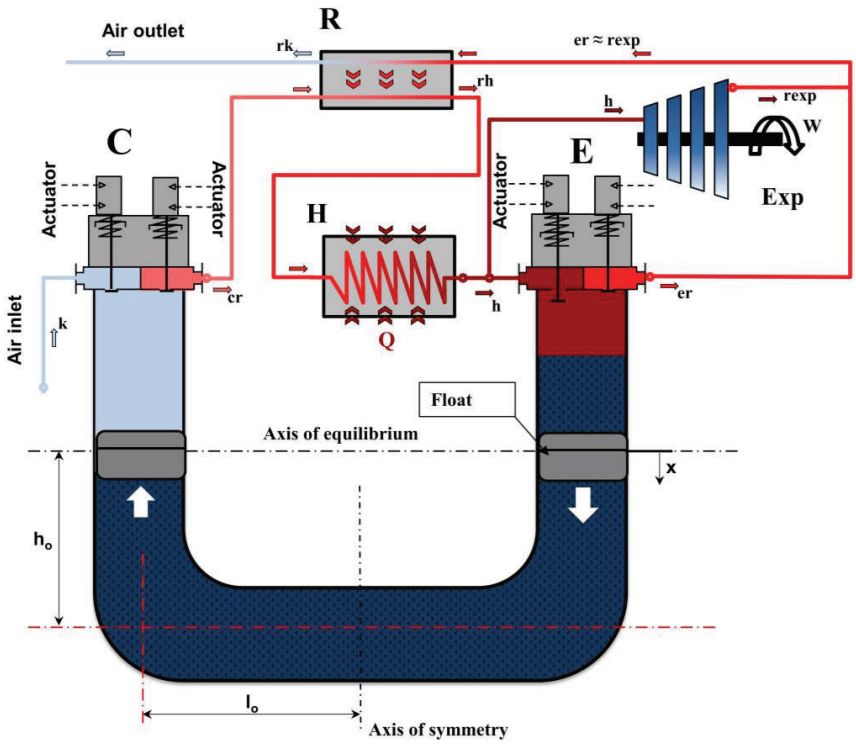

Figure 1. Schematic diagram of the free liquid piston Ericsson engine.

The space between the liquid surface and the cylinder head of one branch is the compression space C, while the same space is the expansion space E in the other branch. The configuration studied operates in an open cycle, with atmospheric air entering the compression space, being compressed by the liquid piston, then discharged to a heat recovery exchanger R and a heater H (hot source of the cycle) before being introduced into the expansion space E. The hot air expanded by the descent of the liquid piston is then discharged to the other branch of the heat recovery exchanger R, during the ascent of the liquid piston. In the case of the configuration studied, only a part of the air mass flow discharged by the compression space is introduced into the expansion space, the mass flow introduced being such that the expansion work exactly compensates for the compression work. In this configuration, the liquid piston and the compression and expansion spaces it defines are similar to a 'free piston gas generator', like the gas generator of the PESCARA engine [23-24]. The compressed air mass flow not admitted to the expansion space can be used as such, at the outlet of the compression space, the system being then a thermal compressor, or be taken after passing through the heat recovery R and heater H exchangers and be expanded in a machine operating in parallel to the liquid piston expansion space, if the objective is to produce mechanical energy (Figure 1).

2.2. The experimental set-up

Figure 2 shows the schematic diagram of the test bench, while figure 3 shows an overview of the experimental set-up. In order for the system to be tested in 'motored engine' mode, the device (Figure 2) is supplied with compressed air from the lab network (1). The compressed air from the external air compressor first passes through a pressure regulator (2) which allows the bench supply pressure to be adjusted, and then passes through a safety valve (3) which limits the downstream pressure to 3 bar, in order to avoid any risk of bursting the Pyrex tube (11). The valve (4) allows the compressed air in the test rig to be drained. A T-connection allows the expansion cylinder to be supplied from both the external compressor and the compression chamber of the liquid piston engine.

https://doi.org/10.52202/069564-0062

When the valves (1) and (5) are open, the compressed air from the external compressor pressurises the entire high-pressure branch of the device, including the two buffer tanks (8) and (15). The pressure line of the compression cylinder is pressurised and the engine can be started by opening the inlet valve of the expansion cylinder and introducing external compressed air.

When the valve (5) is closed, no more compressed air is introduced from the external compressor. A fluidic circuit is established which allows the bench to operate in "engine mode", i.e. the compressed air leaving the compression cylinder is divided into two flows: one part passes into the cold buffer (8), then through the heating cartridge (14) and the hot buffer tank (15) to be admitted into the expansion cylinder (11), and the other part passes into a back-pressure regulator (7) which makes it possible to keep the upstream pressure constant. The flow of air delivered by this back-pressure regulator can be measured by the float flow meter (6). This measurement allows the available air flow to be assessed for practical applications of the engine, such as the production of compressed air or mechanical power by adding an external expander.

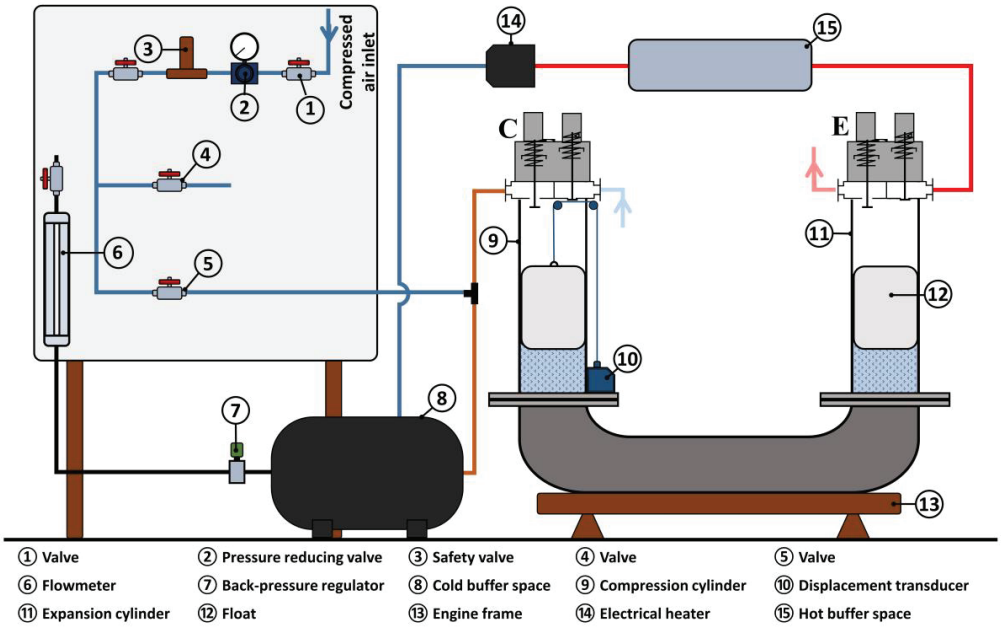

Figure 2. Schematic diagram of the test bench.

The lower part of the liquid piston system is made from commercial high-strength PN 10 pressure PVC pipe. The compression cylinder is made of stainless steel, while the expansion cylinder is made of Pyrex pipe with an external diameter of 180 mm, thickness of 8 mm, length of 500 mm. Two floats, with an external diameter of 156 mm and a length of 250 mm, are inserted in the cylinders. The length of the floats has been chosen to be at least equal to the maximum amplitude of movement of the liquid piston, so that water never licks portions of the wall of the expansion cylinder that would have been in contact with hot air. This reduces the evaporation of water from the liquid piston, as the nominal temperature of introduction of air into the expansion cylinder is 360°C.

Commercial YAMAHA XT500 motorbike engine heads are used to close the compression and expansion cylinders. The valves in these heads are operated by Festo 3/2-way quick-acting 1/4" valves, model MHE4-MS1H3/2G14K, and single-acting pneumatic cylinders, model AEN-40-8APA-S6, also from Festo. These valves are supplied with compressed air from the external air compressor.

The compressed air is heated before it enters the expansion workspace by an electric heating cartridge (item (14) in Figure 2), Osram Sylvania model SureHeat JET 074719, with a maximum power of 8 kW. A control box allows the supply temperature of the expansion cylinder to be set.

The test bench is equipped with K-type thermocouple temperature sensors with a measuring uncertainty of ± 1.5 °C, Keller-Druk PR23S and 23SY pressure sensors which have been calibrated beforehand and have a measuring uncertainty of ± 0.025 bar, and a micro-Epsilon WDS-300-P60-SR-I displacement sensor with a measuring uncertainty of ±0.25 %. This sensor (item (10) in Figure 2) is connected by a pulley system to the float of the compression cylinder. The measurement of the instantaneous pressure in each compression and expansion space is obtained by means of pressure sensors connected to the original location of the spark plugs in the cylinder heads. The sensors are connected to a National Instrument NI cDAQ 9172 modular

chassis data logger controlled by Labview. The sampling rate is 1 kHz. A control box operates the solenoid valves on the valve cylinders based on a comparison between the setpoints and the float position measured by the taut wire sensor.

Figure 3. Overview of the experimental set-up.

3. First experimental results

The first tests did not allow the system to operate autonomously [25], for reasons that will be explained later. The results presented here are therefore all related to a 'motored engine' mode, i.e. with consumption of compressed air from the network. In addition, according to the theoretical results, the displacement amplitude of the free liquid piston increases with the intake pressure of the expansion cylinder. However, in its current version, the amplitude is limited by the length of the tubes and the length of the floats. Therefore, the tests that have been carried out are limited to low pressure ratios. On the other hand, the frequency also depends on the inlet pressure of the expansion cylinder. Experience shows that above a frequency of about 3 Hz, the liquid-air interface no longer behaves satisfactorily. Due to its inertia, the float 'lifts off' from the liquid column and the interface breaks up into a multitude of droplets. For these reasons, the tests are limited to an absolute pressure of 1.6 bar at the inlet of the expansion cylinder.

3.1. Valves setting

The position of the liquid piston is denoted by x. The position $x = 0$ corresponds to the lowest bottom dead centre possible in the expansion cylinder (float on the bottom stop of the cylinder) and the highest top dead centre (TDC) possible in the compression cylinder (float in contact with the top stop of the cylinder). The position $x = 0.3$ m corresponds to the lowest bottom dead centre (BDC) possible in the compression cylinder (float on the bottom stop of the cylinder) and the highest top dead centre possible in the expansion cylinder (float in contact with the top stop of the cylinder).

The compression cylinder valves are supposed to simulate automatic valves, whereas the expansion cylinder valves are actuated valves whose opening and closing are governed by the values of the position of the liquid piston and its direction of movement.

The valves are actuated as follows:

- The inlet valve of the compression cylinder is open when the liquid piston moves downward and the in-cylinder pressure is lower than the atmospheric pressure.
- The outlet valve of the compression cylinder is open when the liquid piston moves upward and the in-cylinder pressure is higher than the pressure in the exhaust pipe.
- The inlet valve of the expansion cylinder is open when the liquid piston moves upward and $x >$ IVO or when the liquid piston moves downward and $x >$ IVC.
- The exhaust valve of the expansion cylinder is open when the liquid piston moves downward and $x <$ EVO or when the liquid piston moves upward and $x >$ IVC.

https://doi.org/10.52202/069564-0062

Figure 4 presents the valves setting of the expansion cylinder. Unless otherwise specified, the results presented here correspond to the following expansion cylinder valves setting:

- IVO = 0.16 m
- IVC = 0.1 m
- EVO = 0.03 m
- EVC = 0.16 m

Theoretically, with this valves setting, there should be an expansion process of the working fluid, since all valves are closed when the liquid piston moves downward from IVC = 0.1 m to EVO = 0.03 m, but there should be no re-compression of the dead space volume since the inlet valve opens at the same time as the exhaust valve closes: EVC = IVO.

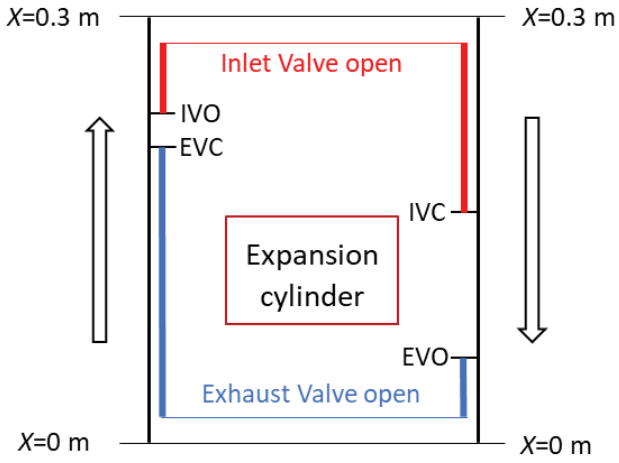

Figure 4. Valves setting for the expansion cylinder.

3.2. Cold tests

3.2.1. Frequency and stroke

Figure 5 shows the theoretical and experimental liquid piston displacement as a function of time, for a test duration of 20 s with a time step of 10^{-3} s. The expansion cylinder inlet pressure is set to 1.3 bar. There is good agreement between the theoretical and experimental data, both in term of frequency (about 2.2 Hz for the experimental and theoretical results) and stroke (about 124 mm for the theoretical results and 105 mm for the experimental ones, that is less than half the maximum possible travel between the stops).

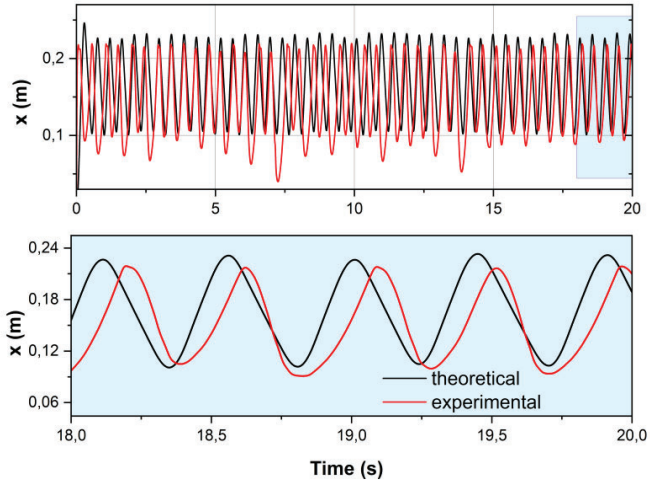

Figure 5. Liquid piston displacement as a function of time.

https://doi.org/10.52202/069564-0062

Figure 6 presents the frequency and the stroke as a function of the expansion cylinder inlet pressure. As the modelling has shown, it is not possible to vary the expansion cylinder inlet pressure without adjusting the valves setting. The experimental results shown in figure 6 are obtained by varying the pressure of the air admitted into the expansion cylinder from 1.15 to 1.5 bar. For the theoretical results, the model has been re-run, with the experimentally imposed pressure and valves setting, to allow comparison between the experimental and theoretical data. It can be seen that the theoretical frequency and stroke increases nearly linearly with the expansion cylinder inlet pressure. The experimental values are in fairly good agreement with the theoretical values, and the differences can be attributed largely to the fact that the experimental instantaneous pressure in the expansion cylinder is far from the theoretical pressure, due to pressure losses in the intake line, as will be shown below. The same applies to the compression cylinder, where the exhaust valve generates large pressure losses.

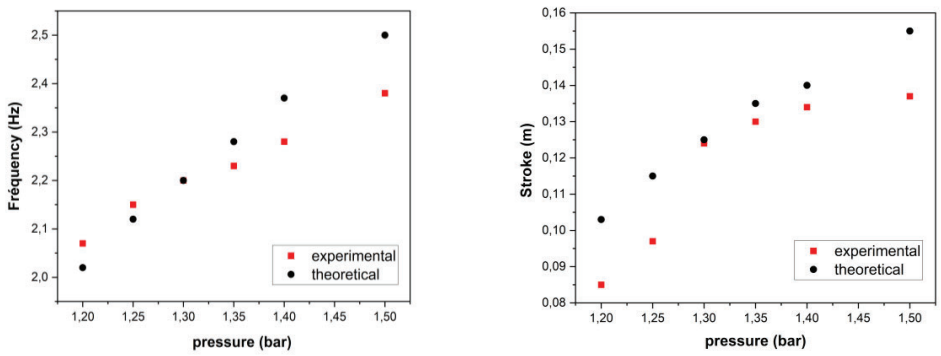

Figure 6. Frequency and stroke as a function of the expansion cylinder inlet pressure.

3.2.2. Instantaneous pressures

Figure 7 presents the instantaneous pressures measured at the expansion cylinder inlet (*p_admE*), in the compression cylinder (*p_C*), at the compression cylinder outlet (*p_echC*), in the expansion cylinder (*p_E*) and at the heater cartridge inlet (*p_Cart*), as a function of time for different expansion cylinder inlet pressures.

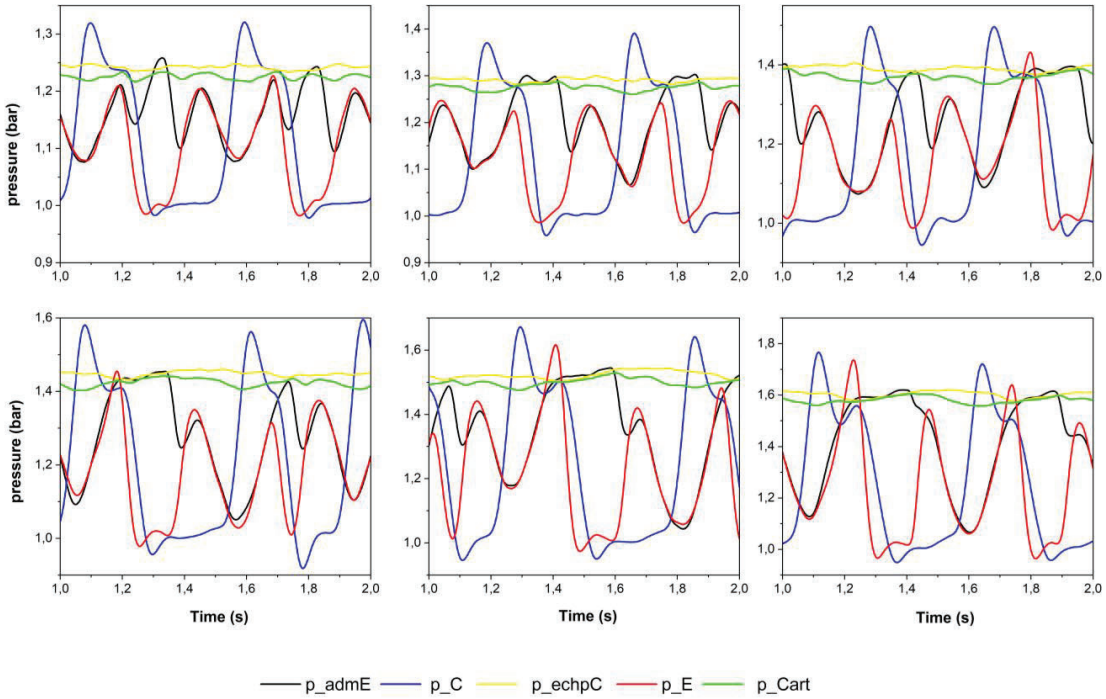

Figure 7. Instantaneous pressures as a function of time for different expansion cylinder inlet pressures.

It can be seen in Figure 7 that the pressures at the inlet of the heater cartridge *p_Cart* and at the outlet of the compression cylinder *p_echC* are almost constant, and almost identical, the pressure at the inlet of the

https://doi.org/10.52202/069564-0062

cartridge being slightly lower due to the greater pressure drop in the connecting pipe. In contrast, the expansion cylinder inlet pressure *p_admE*, which is supposed to be constant in the model, varies greatly when the inlet valve opens and closes. This is due to the high pressure drop generated by the pipe that connects the hot buffer tank to the expansion cylinder head. This line 'deflates' when the inlet valve opens and 're-inflates' to the cartridge inlet pressure when the inlet valve closes. The higher the pressure imposed by the compressed air in the high-pressure branch, the more pronounced this phenomenon becomes. This high pressure drop is the main reason why the engine has not yet been able to operate autonomously, without energy supply from the compressed air network. During the opening phases of the expansion cylinder intake valve, the pressure *p_E* in the cylinder is almost identical to the pressure in the intake pipe *p_admE*, proving that the pressure losses in the intake valve are negligible. However, these pressures are far from being equal to the constant pressure *p_Cart* as assumed in the model.

As far as the compression cylinder is concerned, it can be seen that when the free liquid piston moves up towards its top dead centre, the pressure in the cylinder *p_C* exceeds the pressure in the exhaust pipe *p_echpC* even though the exhaust valve is open, which indicates that the pressure losses generated by this valve are too high under these operating conditions.

3.2.3. In-cylinder pressures

Figure 8 presents the liquid piston displacement, the state of the valves (1 = open, 0 = closed) and pressure in the expansion cylinder as a function of time. For the valves setting considered, it can be seen that there is a time lag between the closing of the intake valve and the moment when the piston reaches its bottom dead centre. This should lead to an expansion of the fluid in the cylinder, which does not seem to be systematically observed. Similarly, it is also observed that the pressure in the cylinder increases when the liquid piston rises, while the exhaust valve is open, which seems to indicate that the exhaust valve generates significant pressure losses.

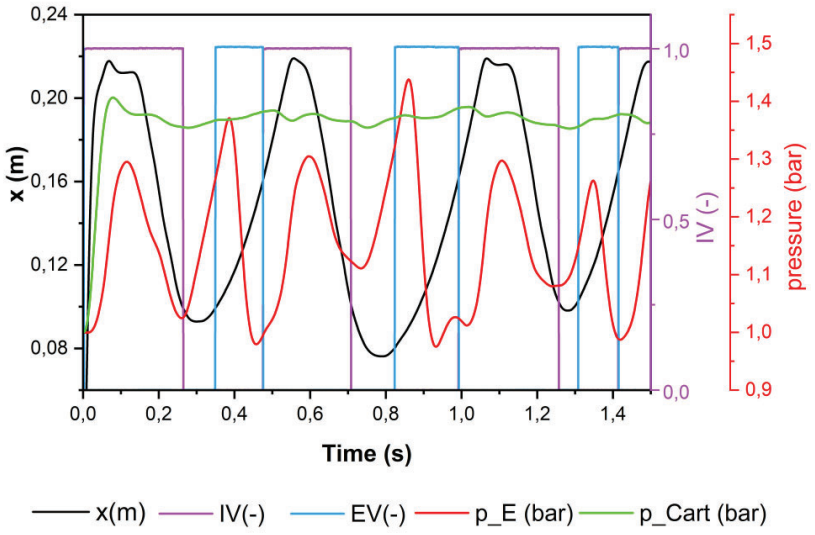

Figure 8. Liquid piston displacement, state of the valves and pressure in the expansion cylinder.

Figure 9 compares the experimental and theoretical pressure evolutions in the compression cylinder (Figure 9 (a)) and in the expansion cylinder (Figure 9 (b)). For the compression cylinder, it can be seen that the experimental pressure is slightly higher than the simulation pressure during the discharge phase, with a peak that is due to pressure drops around the exhaust valve. For the expansion cylinder (Figure 9 (b)), the theoretical results predict isobaric inlet, then isentropic expansion, followed by isobaric outlet and finally isentropic dead volume recompression. As mentioned earlier, the evolution of the experimental pressure *p_E* is significantly different, due to the pressure losses in the inlet line and in the valves, and the time needed for the complete opening and closing of these valves. Despite these problems, it can be seen that the theoretical cycle time corresponds to the experimental cycle time.

https://doi.org/10.52202/069564-0062

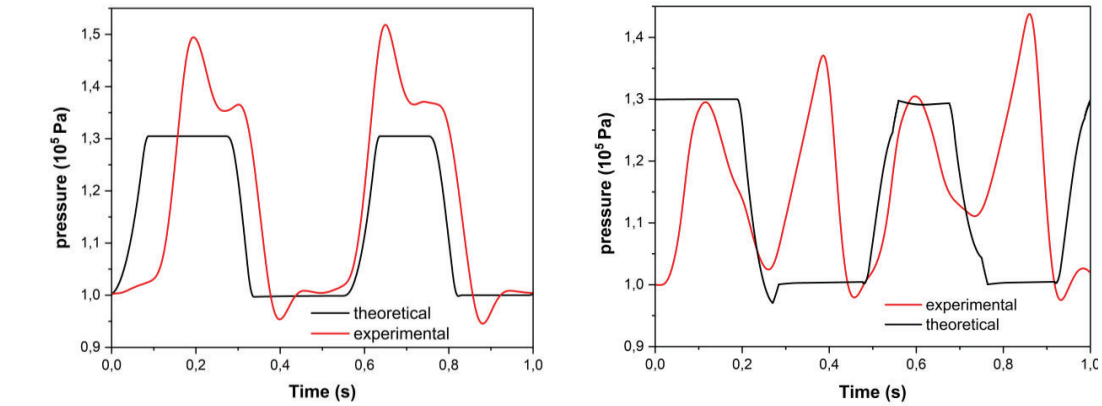

(a) (b)

Figure 9. Instantaneous pressure in the compression cylinder (a) and the expansion cylinder (b).

3.2.4. Indicator diagrams

Figure 10 presents the (*p, V*) indicator diagram for the compression (blue) and expansion (red) cylinder. The area included in the closed curve of the (*p, V*) diagram corresponds to the work of the pressure forces on the liquid piston. A clockwise loop corresponds to a negative work, meaning that the working fluid produces mechanical work on the liquid piston, while a counter-clockwise loop corresponds to a positive work, meaning that the working fluid receives mechanical work from the liquid piston. Obviously, the two diagrams do not resemble the theoretical diagrams composed of almost isobaric and isentropic transformations. Normally, the compression cylinder indicator diagram should be a single counter-clockwise loop and the expansion cylinder indicator diagram should be an identical but clockwise loop.

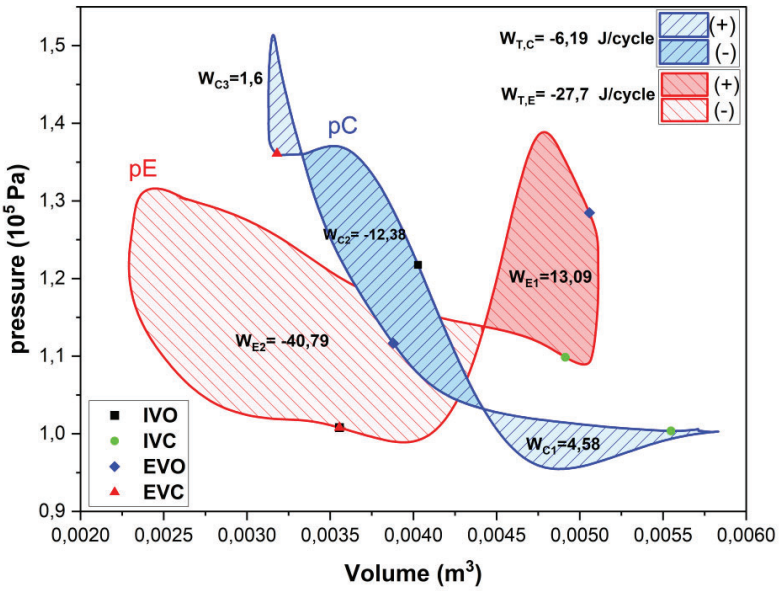

Figure 10. Compression (blue) and expansion (red) cylinder indicator diagram.

Experimentally, it can be seen that the working fluid in the compression cylinder globally gives up work to the liquid piston and the working fluid in the expansion cylinder receives mechanical work from the liquid piston during some phases of the cycle, around the BDC. There are many reasons for this.

As far as the expansion cylinder is concerned, at the moment when, simultaneously, the exhaust valve closes and the intake valve opens, the pressure *p_E* does indeed increase dramatically but with some delay, meaning that the inlet valve does not open instantaneously. But as the piston descends from its TDC towards its BDC, the pressure *p_E*, which should theoretically remain constant at its maximum value, decreases due to pressure losses in the intake line as mentioned above. When the intake valve closes, there should be an isentropic expansion of the fluid. However, the experimental pressure increases. This is due to the fact that the inlet valve

https://doi.org/10.52202/069564-0062

does not close instantaneously, meaning that compressed air goes on entering the expansion cylinder after the EVC point indicated on the red loop of figure 10. The liquid piston being nearly at rest around the BDC, the pressure increases dramatically. Similarly, when the exhaust valve opens around the BDC, the pressure *p_E* does not drop immediately to the value of atmospheric pressure, as would be expected in the theoretical cycle, but instead begins to rise and then gradually falls. This phenomenon is attributable firstly to the time required for the discharge valve to open fully, as it does not open completely instantaneously at the time shown in the diagrams, and secondly to the pressure drop generated by this valve.

As far as the compression cylinder is concerned, it can be assumed that the exhaust valve does not close instantaneously at the EVC point shown in the diagrams in figure 10. Compressed air would therefore enter the compression cylinder even as the liquid piston begins its stroke towards its BDC, leading to a cycle producing mechanical work instead of a cycle receiving mechanical work. In the case where there is no back pressure at the exit of the compression space (figure 11), the discharge of the compressed air is done towards the atmosphere. In figure 11, it can be seen that the indicator diagram (*p, V*) of the compression cylinder rotates counter-clockwise, which means that mechanical work is absorbed by the working fluid, and the expansion cylinder rotates clockwise, which means that mechanical work is supplied by the working fluid. However, despite the early opening of the compression cylinder exhaust valve, the pressure drops around this valve are significant, as the discharge is at a pressure *p_C* much higher than atmospheric pressure, especially when the piston has a high speed, around its mid-stroke. It can be seen that as the piston approaches its top dead centre, the pressure drop decreases and the pressure *p_C* falls towards atmospheric pressure. The mechanical work supplied by the expansion cylinder is more than twice as great as that absorbed by the compressor and the net work is 16.4 J/cycle at a pressure of just over 1.2 bar. The indicator diagrams of figure 11 confirms what the modelling has predicted, that is the possibility to design a free liquid piston Ericsson engine. Indeed the inertia of the liquid piston allows to achieve the compression of the air in the compression cylinder even when the pressure in the compression is higher than the one in the expansion cylinder, the liquid piston moving against the pressure forces.

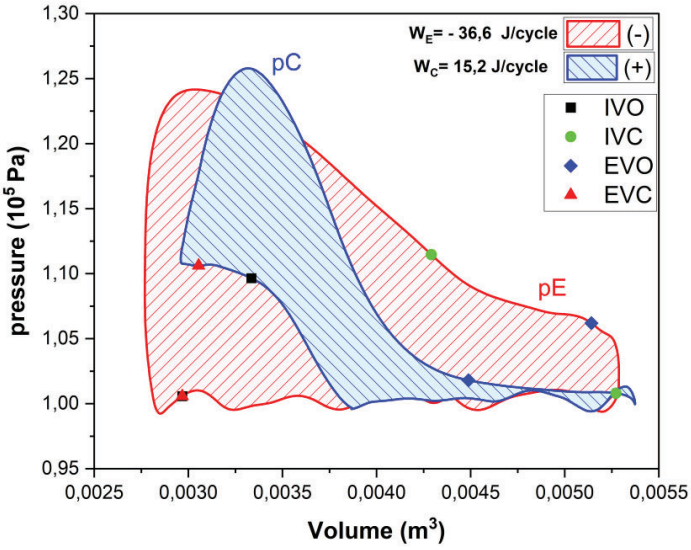

Figure 11. Compression (blue) and expansion (red) cylinder indicator diagram without back-pressure at the compression cylinder outlet.

Finally, it should be mentioned that, although the volumes swept by the liquid piston are obviously identical in the compression and expansion cylinders, the indicator diagrams in figure 10 and figure 11 show that there may be a very slight imbalance between the 2 branches of the liquid piston. The average volume of the compression cylinder is slightly higher than the average volume of the expansion cylinder, which means that the average height of the water in the E-arm of the engine is slightly higher than the average height in the C-arm.

https://doi.org/10.52202/069564-0062

3.3. Hot tests

Different tests were carried out at hot temperatures, up to 200°C.

The results of the experimental tests showed that the temperature does not affect the frequency or the stroke of the free liquid piston, as shown in figure 12, which represents the temporal evolution of the liquid piston displacement for different air inlet temperatures in the expansion cylinder, at the same inlet pressure of 1.3 bar. It can be seen that for the different temperature levels, the amplitude is almost the same. If, for example, we take the displacement for a temperature of 20°C and 190°C, we notice that it is almost the same stroke that is covered by the liquid piston, with the same cycle frequency, as predicted by the theoretical model.

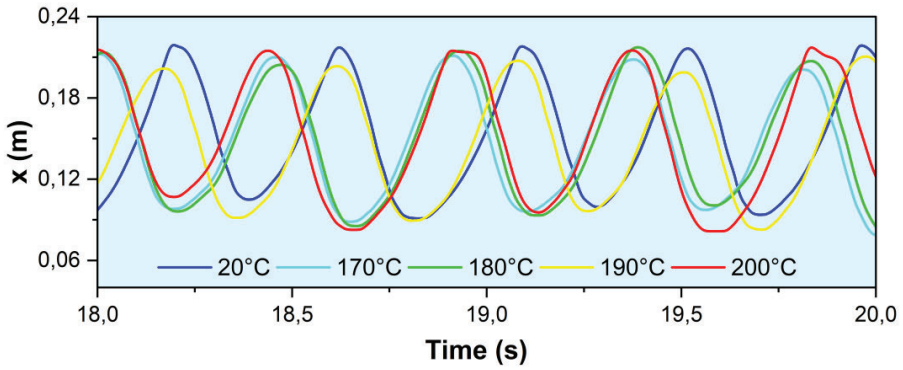

Figure 12. Liquid piston displacement for different inlet temperatures of the expansion cylinder.

The hot tests were carried out in a completely satisfactory manner, without any technical problems. At most, some fogging was observed on the wall of the Pyrex tube, due to the weak evaporation-condensation phenomena of the water in the liquid piston at high temperatures of the air admitted into the expansion cylinder.

4. Conclusion

The results of tests carried out on an original configuration of the Ericsson free liquid piston engine were presented. In its current configuration, the test bench did not allow for 'engine' operation. Tests in 'motored engine' mode using an external compressed air supply showed that it is possible to obtain stable engine operation, provided that the operational parameters (supply pressure, valve opening/closing settings) are carefully chosen. The oscillation frequency of the free piston and its stroke are in good agreement with the results of the theoretical model. The hot tests also demonstrated the good operation of the engine at high temperatures without encountering any technical problems. The examination of the experimental results highlighted the improvements to be made to the test bench.

Nomenclature

IV	state of the inlet valve of the expansion cylinder
IVC	inlet valve closure
IVO	inlet valve opening
EV	state of the exhaust valve of the expansion cylinder
EVC	exhaust valve closure
EVO	exhaust valve opening
p_admE	instantaneous pressure at the inlet of the expansion cylinder, bar
p_C	instantaneous pressure in the compression cylinder, bar
p_Cart	instantaneous pressure at the electrical heater inlet, bar
p_E	instantaneous pressure in the expansion cylinder, bar
p_echpC	instantaneous pressure at the outlet of the compression cylinder, bar
x	liquid piston instantaneous position, m

Subscripts and superscripts

C	compression space
E	expansion space
H	heater
R	heat recovery exchanger
T	external expander

https://doi.org/10.52202/069564-0062

References

[1] Finkelstein T., Organ A. J., Air engines, London: Professional Engineering Publishing Ltd (2001).

[2] Ndamé Ngangué M., Stouffs P., Dynamic simulation of an original Joule cycle liquid pistons hot air Ericsson engine, Energy, 190 (2020), 116293.

[3] Bell M. A., Partridge T., Thermodynamic design of a reciprocating Joule cycle engine, Proc Instn Mech Engrs Part A J Power Energy (2003), vol. 217, pp. 239–246.

[4] Moss R. W., Roskilly A. P., Nanda S. K., Reciprocating Joule-cycle engine for domestic CHP systems, Appl. Energy (2005), vol. 85, pp. 169–185.

[5] Stanciu D., Bădescu V., Solar-driven Joule cycle reciprocating Ericsson engines for small scale applications. From improper operation to high performance, Energy Convers. Manag. (2017), vol. 135, pp. 101–116, doi: 10.1016/j.enconman.2016.12.070.

[6] Komninos N. P., Rogdakis E. D., Design considerations for an Ericsson engine equipped with high-performance gas-to-gas compact heat exchanger: A numerical study, Appl. Therm. Eng. (2018), vol. 133, pp. 749–763, doi: 10.1016/j.applthermaleng.2018.01.078.

[7] Creyx M., Delacourt E., Morin C., Desmet B., Peultier P., Energetic optimization of the performances of a hot air engine for micro-CHP systems working with a Joule or an Ericsson cycle, Energy (2013), vol. 49, no. 1, pp. 229–239, 2013, doi: 10.1016/j.energy.2012.10.061.

[8] Van De Ven R. J. D., Li P. Y., Liquid piston gas compression, Appl. Energy (2009), 86, 2183–2191, doi: 10.1016/j.apenergy.2008.12.001.

[9] Patil V. C., Acharya P., Ro P. I., Experimental investigation of heat transfer in liquid piston compressor, Appl. Therm. Eng. (2018), vol. 146, pp. 169–179, doi: 10.1016/j.applthermaleng.2018.09.121.

[10] Kumar N., Hofacker M., Barth E., Design and Control of a Free-Liquid-Piston Engine Compressor for Compact Robot Power, Vanderbilt Undergrad. Res. J. (2013), vol. 9, pp. 0–6, doi: 10.15695/vurj.v9i0.3796.

[11] Mikalsen R., A. P. Roskilly A. P., A review of free-piston engine history and applications, Appl. Therm. Eng. (2007), 27, 2339–2352, doi: 10.1016/j.applthermaleng.2007.03.015.

[12] Johnson T. A., Leick M. T., Moses R. W., Experimental Evaluation of a Prototype Free Piston Engine - Linear Alternator (FPLA) System, SAE Technical Paper (2016), doi: 10.4271/2016-01-0677.

[13] Xu Z., Chang S., Prototype testing and analysis of a novel internal combustion linear generator integrated power system, Appl. Energy (2010) vol. 87, no. 4, pp. 1342–1348, doi: 10.1016/j.apenergy.2009.08.027.

[14] Jia B., Wu D., Smallbone A., Lawrence C., Paul A., Design, modelling and validation of a linear Joule Engine generator designed for renewable energy sources, Energy Convers. Manag. (2018), vol. 165, pp. 25–34, doi: 10.1016/j.enconman.2018.03.050.

[15] Wang J., Feng H., Zhang Z., Wu L., Yang F., Development of a coupling model and parametric analysis of an opposed free-piston engine linear generator, Appl. Therm. Eng. (2023) vol. 219, doi: 10.1016/j.applthermaleng.2022.119205.

[16] Li H. et al., Development of a Performance Analysis Model for Free-Piston Stirling Power Convertor in Space Nuclear Reactor Power Systems, Energies (2022), vol. 15, no. 3, p. 915, doi: 10.3390/en15030915.

[17] Jiang Z., Yu G., Zhu S., Dai W., Luo E., Advances on a free-piston Stirling engine-based micro-combined heat and power system, Appl. Therm. Eng. (2022), vol. 217, doi: https://doi.org/10.1016/j.applthermaleng.2022.119187.

[18] Zare S.,Tavakolpour‐Saleh A., Free piston Stirling engines: A review, Int. J. Energy Res.(2020), vol. 44, no. 7, pp. 5039‐5070, doi: 10.1002/er.4533.

[19] West C. D., Liquid Piston Stirling Engines, (1983) Van Nostrand Reinhood Company Inc.

[20] Romanelli A., The Fluidyne engine, Am. J. Phys. (2019), vol. 87, no. 1, pp. 33–37, doi: 10.1119/1.5078518.

[21] Chouder R., Stouffs P., Benabdesselam A., Etude d'une nouvelle configuration de moteur Ericsson à piston liquide libre, Actes du Congrès de la Société Française de Thermique (2022), 52.

[22] Chouder R., Benabdesselam A., Stouffs P., Modeling results of a new high performance free liquid piston engine, Energy (2023), 125960, doi:10.1016/j.energy.2022.125960

[23] Pescara R. P., Motor compressor apparatus, Patent N° 1 657 641 (1928).

[24] Pescara C., Générateurs à pistons libres Pescara, Rev. Tech. de l'association des ingénieurs de l'Ecole Breguet, 69 (1963).

[25] Chouder R., Ndamé Nguangué M., Stouffs P., Benabdesselam A., Moteur Ericsson à piston liquide libre : premiers résultats expérimentaux, accepted for presentation, Congrès de la Société Française de Thermique, (2023).